# Programmed necroptosis is upregulated in low-grade myelodysplastic syndromes and may play a role in the pathogenesis

**Jing Zou**[a,1], **Qiong Shi**[a], **Heidi Chen**[b], **Ridas Juskevicius**[c,2], **Sandra S. Zinkel**[a,d,2]

[a]Division of Hematology/Oncology, Department of Medicine, Vanderbilt University Medical Center, Nashville, TN;

[b]Department of Biostatistics, Vanderbilt University Medical Center, Nashville, TN;

[c]Department of Pathology, Microbiology, and Immunology, Vanderbilt University Medical Center, Nashville, TN;

[d]Department of Cell and Developmental Biology, Vanderbilt University Medical Center, Nashville, TN

## Abstract

Myelodysplastic syndrome (MDS) is characterized by persistent cytopenias and evidence of morphologic dysplasia in the bone marrow (BM). Excessive hematopoietic programmed cell death (PCD) and inflammation have been observed in the bone marrow of patients with MDS, and are thought to play a significant role in the pathogenesis of the disease. Necroptosis is a major pathway of PCD that incites inflammation; however, the role of necroptosis in human MDS has not been extensively investigated. To assess PCD status in newly diagnosed MDS, we performed immunofluorescence staining with computational image analysis of formalin-fixed, paraffin-embedded BM core biopsies using cleaved caspase-3 (apoptosis marker) and necroptosis markers (receptor-interacting serine/threonine-protein kinase 1 [RIPK1], phospho-mixed lineage kinase domain-like protein [pMLKL]). Patients with MDS, but not controls without MDS or patients with de novo acute myeloid leukemia, had significantly increased expression of RIPK1 and pMLKL but not cleaved caspase-3, which was most evident in morphologically low-grade MDS (<5% BM blasts) and in MDS with low International Prognostic Scoring System risk score. RIPK1 expression highly correlated with the distribution of CD71$^+$ erythroid precursors but not with CD34$^+$ blast cells. We found that necroptosis is upregulated in early/low-grade MDS

relative to control participants, warranting further study to define the role of necroptosis in the pathogenesis of MDS and as a potential biomarker for the diagnosis of low-grade MDS.

## Graphical Abstract
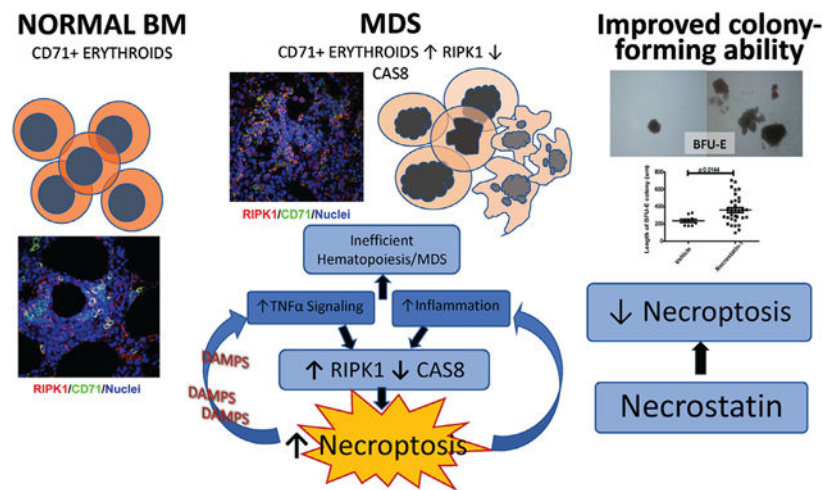


Myelodysplastic syndromes (MDS) are a heterogeneous group of clonal stem cell disorders characterized by ineffective hematopoiesis manifesting as low blood counts and normo- or hypercellular bone marrow (BM) [1–3]. Two prominent features of MDS that have been implicated in the pathogenesis of the disease are increased bone marrow cell death associated with increased inflammatory cytokines such as tumor necrosis factor $a$(TNF-$a$) [4–6]. Early MDS studies described increased hematopoietic cell death, especially in low-risk MDS, (refractory anemia and refractory anemia with ringed sideroblasts) [6] that was proposed to play a significant role in disease pathogenesis [7]. Recently, inflammatory cytokines such as TNF-$a$, which have also been implicated as regulatory cues, have been reported to promote the proliferation and PCD of hematopoietic progenitors in MDS, further implicating an inflammatory process as a pathogenic driver of MDS [4,5,8–10].

Increased programmed cell death (PCD) in early MDS BM studies was interpreted as apoptotic death, based on increased in situ DNA end labeling (TUNEL staining) [11–13]. Apoptosis is driven by proteases called caspases that break down the cytoskeleton to cause collapse of the cell in a mostly immune silent process [14,15]. Recently, necroptosis has been identified as an important programmed cell death (PCD) pathway, which is driven by RIP kinases. In contrast to apoptosis, necroptosis is characterized by premature rupture of the plasma membrane, resulting in the release of damage-associated molecular patterns (DAMPs) that elicit an inflammatory response [16,17].

The most extensively characterized death receptor-induced programmed necroptosis pathway is initiated by ligation of TNF receptor (TNFR1) with TNF-$a$. After ligation, TNFR1 recruits tumor necrosis factor receptor type 1-associated death domain (TRADD), receptor-interacting serine/threonine-protein kinase 1 (RIPK1), TNF receptor-associated factor 2 (TRAF2), and cellular inhibitor of apoptosis protein 1 (cIAP1/2) to form complex I at the plasma membrane. RIPK1 undergoes deubiquitylation to allow association with

Fas-associated protein with death domain (FADD), TRADD, and RIPK3 in the cytosol to form complex II. FADD mediates the recruitment and activation of pro-caspase-8 [18].

Activation of caspase-8 plays a key role in directing whether a cell will undergo apoptosis or necroptosis. Activated caspase-8 can activate effector caspases such as caspase-3 to initiate apoptosis. In addition, activated caspase-8 cleaves and inactivates RIPK1 and RIPK3, thereby preventing necroptosis [19,20]. However, if caspase-8 enzymatic activity is inhibited (by cFLIP), RIPK1 and RIPK3 are stabilized and form the necroptosome [21], allowing interdependent phosphorylation and activation of RIPK1 and RIPK3 within the necroptosome and execution of necroptosis (Figure 1A).

The methods used to detect PCD in early studies do not distinguish between necroptosis and apoptosis. Both apoptotic and necroptotic cells will display increased in situ end labeling, increased terminal deoxynucleotidyl transferase dUTP nick end labeling (*TUNEL*), and increased Annexin V positivity. Increased caspase-3 activity has been noted after ex vivo culture of BM cells from patients with MDS [22] but not when caspase-3 activation is measured directly ex vivo by intracellular flow cytometry, where only a minority of MDS samples displayed evidence of caspase-3 activation [23].

Thus, multiple groups have determined that BM from patients with MDS has a propensity to undergo PCD as measured by methods detecting DNA degradation. However, the signaling pathways regulating this PCD and their role in the pathogenesis of MDS have not been well described. Our laboratory has developed a mouse model in which BM necroptosis is increased, and we found that the mice die of BM failure with the salient characteristics of MDS, including BM hypercellularity and abnormal, dysplastic differentiation of the hematopoietic cells [24], and that levels of RIPK1 and phosphor-mixed lineage kinase domain-like protein (pMLKL), key necroptosis signaling proteins, increased in a small number of samples from patients with MDS.

In this study, we ask whether necroptosis might represent an important cell death mechanism in MDS pathogenesis. In particular we investigate whether this inflammatory type of PCD correlates with MDS subtype, the type of cells expressing necroptotic markers, and the impact of inhibiting necroptosis on normal and MDS cell viability. We also propose that the detection of necroptosis could be a potential diagnostic marker, prognostic indicator, and therapeutic target for MDS.

## METHODS

### Patients and control samples

This study included 28 patients initially diagnosed with MDS between 2006 and 2016 at our institution with no prior disease-modifying treatment and with adequate formalin-fixed, paraffin-embedded (FFPE) BM trephine biopsy tissue.

The initial diagnosis and classification of MDS was made according to the French–American–British (FAB) criteria [25] and 2008 World Health Organization (WHO) classification [26]. A board-certified hematopathologist reviewed samples and laboratory

and clinical data for all enrolled patients and translated the initial diagnoses to the terminology used by the revised 2016 WHO classification [27]. Patients with therapy-related MDS were excluded. The patient diagnoses represented the full spectrum of morphologically low-grade MDS (blasts <5%, $n = 15$) including MDS with single-lineage dysplasia (MDS-SLD), MDS with multilineage dysplasia (MDS-MLD), MDS with ringed sideroblasts (MDS-RS), MDS unclassifiable (MDS-U with <5% blasts). Also included are patient diagnoses representing high-grade MDS (>5% blasts, $n = 13$), including MDS with excess blasts (MDS-EB-1 with 5%–9% blasts and MDS-EB-2 with 10%–19% blasts). The control cases ($n = 29$) were BM specimens from patients with no peripheral cytopenias and no morphologic, immunophenotypic, or genetic abnormalities. Five patients with de novo acute myeloid leukemia (AML) were also included as a control group. Clinical information at presentation and follow-up was retrieved from our electronic medical record system. This study was approved by our institutional review board.

For gene expression analysis, the publicly available Gene Expression Omnibus (GEO) data set (GSE15061) [28] containing data for 164 MDS, 202 AML, and 69 nonleukemia BM samples hybridized to Affymetrix HG-U133 Plus 2.0 GeneChips (subset of the Microarray Innovations in Leukemia [MILE] study) program of the European Leukemia Network (ELN) was analyzed (https://www.ncbi.nlm.nih.gov/geo/query/acc.cgi?acc=GSE15061).

### Cytogenetic analysis and IPSS-R scoring

Detailed experimental procedures are provided in the Supplementary Methods (online only, available at www.exphem.org).

### Formalin-fixed, paraffin-embedded tissue specimens

Detailed experimental procedures are provided in Supplementary Data and Supplementary Figure E1 (online only, available at www.exphem.org).

### Antibodies and immunofluorescence staining

Detailed experimental procedures are provided in the Supplementary Data (online only, available at www.exphem.org).

### Immunofluorescence imaging and computational image analysis

Confocal images were acquired on an Olympus FV-1000 inverted confocal microscope (Olympus, Waltham, MA). Digital images were collected using the microscope in sequential mode with a line average of 4 and a format of $1024 \times 1024$ pixels with 8-bit sensitivity. Fluorescent whole-slide images were acquired on the Aperio Versa 200 automated slide scanner (Leica Biosystems, Nussloch, Germany) for consistent, standardized, and objective imaging and quantification of whole slides. BM tissue cores were imaged at $20 \times$ magnification to a resolution of $0.323 \ \mu$m/pixel. Images were stored on the Digital Image Hub hosted by our institution's DHSR (Digital Histology Shared Resource). Each whole-slide image was segmented into pieces. The protein expression and co-localization were analyzed using CellProfiler software (Broad Institute, Cambridge, MA) [29,30]. A CellProfiler pipeline for statistical analysis was developed (described in Supplementary Figure E2, online only, available at www.exphem.org) to evaluate and measure the

immunofluorescence signals, containing the number, shape, size, and median intensity of signals (RIPK1, pMLKL, cleaved caspase-3, CD34, CD71). Analysis of each slide included at least 5,000 cells.

### Statistical analysis

Detailed experimental procedures are provided in Supplementary Methods (online only, available at www.exphem.org).

## RESULTS

### Expression of *CASPASE-8* was lower in those with MDS as compared those with healthy BM in the MILE study data set

We first evaluated gene expression among PCD pathways in the publicly available microarray data set GSE15061 [31], which includes BM samples from 164 patients with MDS versus 68 individuals without MDS. We employed overrepresentation analysis using the hypergeometric test to measure the percentage of genes in cell death pathways that have differential expression (i.e., statistically significant changes in gene expression between patients with MDS and individuals without MDS) [32]. Interestingly, we noted that *CASPASE-8* expression was significantly lower in the BM of 164 patients with MDS versus the BM of 68 individuals without MDS ($p = 0.0000109$) (Figure 1B) [33]. This finding, in the light of the existing evidence for inflammation in MDS, suggested the possibility that apoptosis may not be the predominant cell death pathway activated in MDS, warranting further investigation.

### Expression of RIPK1 and pMLKL, but not caspase-3, was increased in patients with MDS relative to control participants or those with de novo AML

To investigate PCD pathways in MDS further, we evaluated expression of RIPK1 and pMLKL (necroptosis) and activated caspase-3 (apoptosis) in MDS BM patient samples obtained at first diagnosis. In our patient cohort, FFPE BM biopsy samples from 28 patients with a new diagnosis of MDS, 29 control patients, and 5 de novo patients with AML were analyzed. The clinicopathologic profile of these patients is summarized in Table 1 and Supplementary Table E3 (online only, available at www.exphem.org).

CellProfiler image analysis revealed that the proportion of RIPK1-positive cells in our cohort of patients with MDS was significantly higher as compared with those of the control group (mean 29.21% vs. 8.243%, $p < 0.0001$) and the de novo AML group (29.21% vs.1.983%, $p = 0.008$) (Figure 2A).

To determine whether increased RIPK1 was simply a feature of normal aging, we compared the expression of RIPK1 in the older subject population (age >60). RIPK1 expression was significantly higher in MDS than in control participants in this older group (Supplementary Figure E4, online only, available at www.exphem.org). Furthermore, the proportion of pMLKL (the executioner of necroptosis)-positive cells in the MDS group was significantly higher compared with that of the control group (12.86% vs. 5.26%, $p = 0.031$) (Figure 2B). RIPK3 staining also revealed increased expression in MDS (Supplementary Figure E5,

online only, available at www.exphem.org). In contrast, the amount of staining for cleaved caspase-3, the executioner of apoptosis, did not differ among the three groups (Figure 2C).

**RIPK1-positive cells were highly correlated with CD71⁺ but not CD34⁺ cells**

The RIPK1⁺ cells were mononuclear, which in MDS cases were primarily arranged in clusters or in an interstitially diffuse distribution, and in AML cases, were individually scattered cells (Figure 3A). In addition, the distribution of RIPK1⁺ cells resembled erythroid islands, which in BM biopsy specimens consist of cell clusters with small, dark round nuclei in proximity to the marrow sinusoids in some areas surrounding hemosiderin-laden macrophages (Figure 3B).

Lineage-specific immunofluorescence cell surface markers revealed that in both control and MDS samples, RIPK1⁺ cells did not exhibit CD34 expression (Figure 3C). In contrast, RIPK1 and CD71 were highly co-localized in both control and MDS cases (Figure 3D,E). Our CellProfiler software analysis of the multiplex immunofluorescence images reported six parameters: number of RIPK1⁺ cells, number of CD71⁺ cells, number of double-positive cells, number of double-negative cells, intensity of CD71 signal, and intensity of RIPK1 signal. Correlational analysis was performed between CD71 and RIPK1 staining in the control and MDS groups. For the control group, the correlation between CD71 and RIPK1 was positive ($R^2 = 0.6599$, Pearson's $R = 0.8123$, $p < 0.0001$). For the MDS group, the correlation between CD71 and RIPK1 was even more significant ($R^2 = 0.8466$, Pearson's $R = 0.9201$, $p < 0.0001$). To test the difference in correlation between the control and MDS groups, we used the statistical analysis procedure developed by Fisher in 1921 [34]. Using Fisher's method, we found a significant difference between control participants and patients with MDS ($p < 0.0001$), indicating that the correlation of CD71 and RIPK1 expression within the MDS group is significantly higher than that in the control group. Specifically, the proportion of RIPK1 and CD71 double- positive cells was 9% in the control patients and 30% in the MDS cases. Furthermore, we observed that >80% of RIPK1⁺ cells were also expressing CD71, consistent with the erythroid lineage (Figure 3F). These results indicate that erythroblasts exhibit increased necroptosis signaling in MDS.

**Treatment with necrostatin-1 enhances colony formation of MDS patient BM**

Given the increased RIPK1 observed in MDS BM, we asked whether culture in the presence of necrostatin-1 (Nec-1) would confer a survival advantage to primary MDS BM cells. This is particularly important as MDS primary cells are notoriously difficult to grow in culture. We cultured BM aspirate from a patient diagnosed with MDS-MLD in methylcellulose for 12 days in the presence or absence of Nec-1 and quantified colony formation. We observe all colony-forming unit types in marrow treated with Nec-1 with the exception of colony-forming unit—granulocyte, erythroid, macrophage, megakaryocyte (CFU-GEMM) (Figure 4A). In particular, we find that burst-forming colony unit–erythroid (BFU-E) colonies grew significantly larger (the longest diameter of BFU-E colonies is presented) in the presence of Nec-1 ($p = 0.0144$) (Figure 4B), reflecting an increased number of cells. Although we observed a trend toward an increase in all colony types, we specifically saw an increase in the total number ($p = 0.0299$) and percentage ($p = 0.0420$) of BFU-E (Figure 4C). Overall, these results indicate improved survival of MDS erythroid progenitor cells in the setting

of RIPK1 inhibition, consistent with our finding that RIPK1 is highly expressed in CD71^{+} erythroid precursors.

Lastly, we evaluated the impact of Nec-1 on normal patient colony formation. We treated isolated mononuclear cells from apheresis samples of patients with lipopolysaccharide (LPS) and cultured them in the presence or absence of Nec-1. We found that cells treated with LPS had increased RIPK1 and pMLKL expression (Supplementary Figure E6A,B, online only, available at www.exphem.org). In the presence of Nec-1 we found an increase in the number of BFU-E ($p = 0.033$) and an overall increased number of CFUs ($p = 0.0448$) (Figure 4D,E) as well as decreased RIPK1 and pMLKL (Supplementary Figure E6A,B, online only, available at www.exphem.org). This suggests that BFU-E cells are particularly sensitive to inflammatory stimuli that result in necroptotic cell death.

## Expression of RIPK1 and pMLKL was increased in those with low-grade MDS morphology and low IPSS-R scores

Next, we divided our MDS cohort into low-grade (BM blasts <5%) and high-grade (BM blasts 5%–19%) groups. The proportion of RIPK1-positive cells in low-grade MDS was significantly higher than that in the control group (27.93% vs. 7.669%, $p = 0.0003$). The proportion of RIPK1-positive cells was significantly higher in high-grade MDS (20.20% vs. 7.669%, $p = 0.0018$) relative to control participants ($p = 0.0693$). RIPK1 staining in de novo AML was less frequent than in the low-grade MDS ($p = 0.013$), high-grade MDS ($p = 0.0157$), or control ($p = 0.0072$) group (Figure 5A,B).

Because the IPSS-R scoring system has been used to guide clinical the decision making and prognosis of patients with MDS, our MDS patient cohort was also divided into low-risk (IPSS-R score <4.5) and high-risk (IPSS-R score >4.5) groups. We observed a similar trend in that the proportion of RIPK1-positive cells in low-risk MDS (26.32%) was also significantly higher than in the control group ($p = 0.0006$) and the de novo AML group ($p = 0.0154$). Similarly, significantly higher expression ($p = 0.0373$) of pMLKL was observed in low-risk MDS (11.30%) than in the control (5.35%) and de novo AML (1.74%) groups ($p = 0.0581$). We observed no difference in the proportion of caspase-3-positive cells among the control, MDS (low/high morphologic grade or low/high IPSS-R risk) and de novo AML groups (Figure 5B).

Given that RIPK1 expression corresponded to low-grade and low-IPSS-R-risk MDS, we were interested to know if in an individual patient with progressive disease, we would observe changes in RIPK1 expression. FFPE bone marrow biopsies were obtained from a patient initially diagnosed with MDS-RS that eventually progressed to AML. Compared with a control sample, we observed a substantial amount of RIPK1 positivity in low-grade MDS. As this patient progressed to MDS-EB-1 and ultimately AML, we observed a decrease in RIPK1 expression (Figure 5C). Thus, in a single patient we observed that low-grade MDS has higher RIPK1 as compared with samples representing progression to higher-grade disease.

**The necroptosis pathway is more activated in MDS than AML in the MILE study data set**

We further evaluated the expression of PCD pathway genes among 164 patients with MDS versus 202 patients with AML and found a significant difference ($p = 0.004$) in expression between these groups [28]. The gene expression fold change among the apoptosis and necroptosis pathways was presented as a $\log_2$ value (Figure 6A). Genes involved in the upstream signaling processes of TNFR were increased in MDS, including *TNFR1* and members of its induced formation of receptor-bound complex I. In complex II, FADD, RIPK1, and RIPK3 were increased, and *CASPASE-8* was suppressed. Caspase-8 is commonly recognized as one of the initiator caspases in both the extrinsic and intrinsic apoptosis pathways. In addition, activated caspase-8 cleaves and inactivates RIPK1 and RIPK3, thereby preventing necroptosis [35]. We found that in MDS versus AML, *CASPASE-8* expression was decreased, and *RIPK1, RIPK3*, and *MLKL* were increased, consistent with increased necroptosis signaling. In contrast, beginning with *CASPASE-8* suppression, the intrinsic apoptosis pathway, including the pro-apoptotic members of the *BCL-2* family (*BAD, BAX, and BID*), cytochrome c and *CASPASE-9* were decreased (Figure 6B). Important additional regulation of these pathways occurs at the post translational level, however, considered in light of our assessment of *RIPK1* and *pMLKL* in FFPE samples, these results provide additional support for the premise that PCD, predominantly programmed necroptosis, is increased in the bone marrow samples from patients with MDS [28].

## DISCUSSION

Early studies of MDS BM have found excessive hematopoietic PCD, which is thought to play a significant role in the pathogenesis of the disease [12,36]. These early studies did not distinguish between apoptotic and necroptotic cell death, and most were performed on isolated hematopoietic cells, and therefore may not exhibit cell death that represents the in vivo status of MDS BM [37]. In addition, our analysis of the publicly available gene expression microarray data (GSE15061) indicated that expression of the initiator of apoptosis, *CASPASE-8*, was significantly lower in MDS relative to healthy bone marrow. Our immunofluorescence staining results revealed that the apoptosis executioner, cleaved (activated) caspase-3, was not increased in BM biopsy specimens from patients with MDS as compared with control or de novo AML samples. In addition, antiapoptotic agents such as erythropoietin and granulocyte colony-stimulating factor (G-CSF) exhibit limited durable effects in MDS [38].

In contrast to the insignificant detection of cleaved caspase-3, we found a markedly different pattern of expression for the necroptosis signaling proteins RIPK1 and pMLKL in the same patient groups. The RIPK1–RIPK3–MLKL complex has been well established as a key mediator of the necroptosis pathway [35]. The small molecule inhibitor Nec-1 inhibits necroptotic but not apoptotic death through pharmacologic inhibition of the kinase domain of RIPK1, further demonstrating the importance of RIPK1 in programmed necroptosis [39]. In our cohort, RIPK1 expression was significantly increased in MDS BM relative to BM of control patients or patients with AML. Higher RIPK1 expression was seen in MDS BM with low-grade morphology/low IPSS-R scores, and the expression pattern was similar to

that of pMLKL. To our knowledge, this is the first comprehensive evaluation of the level of programmed necrosis (necroptosis) versus apoptosis in BM samples from patients with MDS.

It is interesting to consider other scenarios in which necroptosis signaling may be significantly increased in the BM. One such scenario is the setting of increased cell turnover. Cell turnover and cell proliferation have been investigated in MDS and myeloproliferative neoplasms (MPNs) by directly measuring Ki-67 [40] and LDH [41]. These studies revealed decreased erythrocyte proliferation in MDS and increased erythrocyte proliferation in MPNs. LDH was found to be elevated and of prognostic significance in the MPN primary myelofibrosis (PMF). As we see increased RIPK1 in early MDS, where KI67 has been found to be decreased relative to normal marrow, we would not expect that the increased RIPK1 could be attributed to increased turnover in MDS bone marrows. Hemolytic anemia is another distinct scenario with increased cell turnover. These anemias are associated with increased erythrocyte destruction and resultant activation of inflammatory cytokines, and we would hypothesize that RIPK1 may be increased in these settings. It would be very interesting and important to evaluate the necroptosis pathway at the protein level in MPNs and other bone marrow disorders characterized by increased turnover or increased inflammation.

Several studies have reported increased pyroptosis, a form of inflammatory cell death that is executed through the NLRP3 inflammasome in a small number of samples from patients with MDS (five low-risk MDS samples and five high-risk MDS samples) [42]. Emerging understanding of inflammatory PCD pathways has elucidated significant crosstalk [43], and we would predict that the two modes of inflammatory cell death would coexist within the bone marrow microenvironment, and both may participate in a feed-forward inflammatory process that culminates in bone marrow failure. On the basis of our studies in a mouse model with unrestrained bone marrow necroptosis, the presence of necroptotic cells will induce cytokine production in the bone marrow microenvironment through production of DAMPs, which may activate the inflammasome, resulting in a feed-forward inflammatory process that culminates in bone marrow failure [24]. TNF-$\alpha$ has been reported to activate the NLRP3 inflammasome in cultured BMDMs [44]. Notably, the impact of activating the NLRP3 inflammasome through Tak1 on mouse bone marrow myeloid cells can be partially but not completely rescued by inactivating RIPK1 kinase activity [44], consistent with either a direct or an indirect role for RIPK1 in NLRP3 inflammasome activity. RIPK3 may also activate the inflammasome [45], further suggesting crosstalk between these two pathways and underscoring the importance of studies within the bone marrow microenvironment, a strength of our study.

In addition, it is important to note the limitations of immunofluorescence staining of FFPE bone marrow sections. Because of the required decalcification process, there is potential for destruction of epitopes. We have carefully evaluated this possibility for RIPK1, caspase-3, and pMLKL (Supplementary Figure E1, online only, available at www.exphem.org) and find no difference in staining with or without decalcification. We are further limited by the availability of reagents and bone marrow biopsy material for a more comprehensive assessment of cell death pathways and related clinical conditions.

Our study evaluates PCD in the context of the hematopoietic niche and the associated topographic relationship between hematopoietic cells and marrow stromal cells on the entire slide of each patients' BM core biopsy. This is information that is lost from studies in which MDS hematopoietic cells are removed from their niche for analysis. Our multiplex immunofluorescence staining revealed that RIPK1^{+} cell clusters exhibited high expression of CD71 but not CD34. These results are consistent with increased necroptosis signaling, which is most pronounced in the erythroid progenitors.

Importantly, we sought to determine if we could improve viability of cultured MDS marrow in the presence of the RIPK1 inhibitor Nec-1. Consistent with the high levels of RIPK1 positivity observed in CD71 erythroid progenitors, we observe increased size and number of burst-forming unit—erythroid colonies (BFU-E) in the presence Nec-1 compared with vehicle-treated cells. We also found that normal apheresis samples are susceptible to RIPK1 upregulation with LPS stimulation and that BFU-E colony numbers improved with Nec-1 treatment. These data are consistent with a role for necroptosis in MDS cell viability, particularly erythroid cells.

Interestingly, based on the public gene expression microarray data (GSE15061) the most significant difference between apoptosis and necroptosis PCD pathways was lower expression of *CASPASE-8* in patients with MDS as compared with those with AML and control participants (Figure 6). Caspase-8 links the intrinsic and extrinsic apoptotic pathways through cleavage of the pro-apoptotic *BCL-2* family member *BID* [46]. Recent data also implicate caspase-8 as a key controller of the apoptotic versus necroptotic death decision [47]. We further found additional genes in the intrinsic apoptosis pathway to be suppressed, including the pro-apoptotic members of the *BCL-2* family (*BAD, BAX*, and *BID*), *CYTOCHROME C*, and *CASPASE-9*. In contrast, we found that expression of genes in the necroptosis pathway (*RIPK1–RIPK3–MLKL*) was increased in MDS relative to AML. It is important to note several limitations of the MILE data set analysis with respect to PCD pathways. PCD is regulated to a significant extent by posttranslational modification of PCD genes. In addition, the MILE data set does not indicate low-risk versus high-risk MDS cases. Nonetheless, these gene expression changes provide some independent evidence that the necroptosis pathway is upregulated in MDS. Taken together with our study, these results indicate that necroptosis, but not apoptosis, is upregulated in MDS, especially low-grade/early MDS. We thus propose that necroptosis and not apoptosis is a prominent mechanism of PCD in MDS and suggest that further study of RIPK1 expression as a biomarker for the diagnosis and prognosis of early MDS is warranted.

## Supplementary Material

Refer to Web version on PubMed Central for supplementary material.

## Acknowledgments

(www.mc.vanderbilt.edu/dhsr). Experiments were performed in part using the Vanderbilt Cell Imaging Shared Resource and Translational Pathology Shared Resource.

## REFERENCES

1. Cazzola M, Malcovati L. Myelodysplastic syndromes—Coping with ineffective hematopoiesis. N Engl J Med 2005;352:536–8. [PubMed: 15703418]

2. Malcovati L, Nimer SD. Myelodysplastic syndromes: Diagnosis and staging. Cancer Control 2008;15(Suppl):4–13. [PubMed: 18813205]

3. Raza A, Galili N. The genetic basis of phenotypic heterogeneity in myelodysplastic syndromes. Nat Rev Cancer 2012;12:849–59. [PubMed: 23175121]

4. Kitagawa M, Saito I, Kuwata T, et al. Overexpression of tumor necrosis factor (TNF)-alpha and interferon (IFN)-gamma by bone marrow cells from patients with myelodysplastic syndromes. Leukemia 1997;11:2049–54. [PubMed: 9447819]

5. Tsimberidou AM, Estey E, Wen S, et al. The prognostic significance of cytokine levels in newly diagnosed acute myeloid leukemia and high-risk myelodysplastic syndromes. Cancer 2008;113:1605–13. [PubMed: 18683214]

6. Tehranchi R, Invernizzi R, Grandien A, et al. Aberrant mitochondrial iron distribution and maturation arrest characterize early erythroid precursors in low-risk myelodysplastic syndromes. Blood 2005;106:247–53. [PubMed: 15755901]

7. Steensma DP, Tefferi A. The myelodysplastic syndrome(s): a perspective and review highlighting current controversies. Leuk Res 2003;27:95–120. [PubMed: 12526916]

8. Hormaechea-Agulla D, Matatall KA, Le DT, et al. Chronic infection drives Dnmt3a-loss-of-function clonal hematopoiesis via IFNgamma signaling. Cell Stem Cell 2021;28:1428–42. [PubMed: 33743191]

9. Muto T, Walker CS, Choi K, et al. Adaptive response to inflammation contributes to sustained myelopoiesis and confers a competitive advantage in myelodysplastic syndrome HSCs. Nat Immunol 2020;21:535–45. [PubMed: 32313245]

10. Cai Z, Kotzin JJ, Ramdas B, et al. Inhibition of inflammatory signaling in Tet2 mutant preleukemic cells mitigates stress-induced abnormalities and clonal hematopoiesis. Cell Stem Cell 2018;23:833–849.e5. [PubMed: 30526882]

11. Raza A, Gezer S, Mundle S, et al. Apoptosis in bone marrow biopsy samples involving stromal and hematopoietic cells in 50 patients with myelodysplastic syndromes. Blood 1995;86:268–76. [PubMed: 7795232]

12. Shetty V, Mundle S, Alvi S, et al. Measurement of apoptosis, proliferation and three cytokines in 46 patients with myelodysplastic syndromes. Leuk Res 1996;20:891–900. [PubMed: 9009245]

13. Kerbauy DB, Deeg HJ. Apoptosis and antiapoptotic mechanisms in the progression of myelodysplastic syndrome. Exp Hematol 2007;35:1739–46. [PubMed: 17976524]

14. Bogdanovic AD, Jankovic GM, Colovic MD, Trpinac DP, Bumbasirevic VZ. Apoptosis in bone marrow of myelodysplastic syndrome patients. Blood 1996;87:3064. [PubMed: 8639933]

15. Shetty V, Hussaini S, Alvi S, et al. Excessive apoptosis, increased phagocytosis, nuclear inclusion bodies and cylindrical confronting cisternae in bone marrow biopsies of myelodysplastic syndrome patients. Br J Haematol 2002;116:817–25. [PubMed: 11886386]

16. Galluzzi L, Kepp O, Kroemer G. RIP kinases initiate programmed necrosis. J Mol Cell Biol 2009;1:8–10. [PubMed: 19679643]

17. Sun L, Wang H, Wang Z, et al. Mixed lineage kinase domain-like protein mediates necrosis signaling downstream of RIP3 kinase. Cell 2012; 148:213–27. [PubMed: 22265413]

18. Kaczmarek A, Vandenabeele P, Krysko DV. Necroptosis: the release of damage-associated molecular patterns and its physiological relevance. Immunity 2013;38:209–23. [PubMed: 23438821]

19. Lalaoui N, Boyden SE, Oda H, et al. Mutations that prevent caspase cleavage of RIPK1 cause autoinflammatory disease. Nature 2020;577:103–8. [PubMed: 31827281]

20. Newton K, Wickliffe KE, Dugger DL, et al. Cleavage of RIPK1 by caspase-8 is crucial for limiting apoptosis and necroptosis. Nature 2019;574:428–31. [PubMed: 31511692]

21. Feltham R, Vince JE, Lawlor KE. Caspase-8: not so silently deadly. Clin Transl Immunology 2017;6:e124. [PubMed: 28197335]

22. Mundle S, Venugopal P, Shetty V, et al. The relative extent and propensity of CD34+ vs. CD34– cells to undergo apoptosis in myelodysplastic marrows. Int J Hematol 1999;69:152–9. [PubMed: 10222652]

23. Spinelli E, Caporale R, Buchi F, et al. Distinct signal transduction abnormalities and erythropoietin response in bone marrow hematopoietic cell subpopulations of myelodysplastic syndrome patients. Clin Cancer Res 2012;18:3079–89. [PubMed: 22496271]

24. Wagner PN, Shi Q, Salisbury-Ruf CT, et al. Increased Ripk1-mediated bone marrow necroptosis leads to myelodysplasia and bone marrow failure in mice. Blood 2019;133:107–20. [PubMed: 30413413]

25. Bennett JM, Catovsky D, Daniel MT, et al. Proposals for the classification of the myelodysplastic syndromes. Br J Haematol 1982;51: 189–99. [PubMed: 6952920]

26. Vardiman JW, Thiele J, Arber DA, et al. The 2008 revision of the World Health Organization (WHO) classification of myeloid neoplasms and acute leukemia: rationale and important changes. Blood 2009;114:937–51. [PubMed: 19357394]

27. Swerdlow SH C E, Harris NL, Jaffe ES, Pileri SA, Stein H, Thiele J, eds. WHO Classification of Tumours of Haematopoietic and Lymphoid Tissues, revised 4th ed, Lyon: IARC; 2017.

28. Labaj W, Papiez A, Polanski A, Polanska J. Comprehensive analysis of MILE gene expression data set advances discovery of leukaemia type and subtype biomarkers. Interdiscip Sci 2017;9:24–35. [PubMed: 28303531]

29. Soliman K CellProfiler: Novel automated image segmentation procedure for super-resolution microscopy. Biol Proced Online 2015;17:11. [PubMed: 26251640]

30. Carpenter AE, Jones TR, Lamprecht MR, et al. CellProfiler: image analysis software for identifying and quantifying cell phenotypes. Genome Biol 2006;7:R100. [PubMed: 17076895]

31. Mills KI, Kohlmann A, Williams PM, et al. Microarray-based classifiers and prognosis models identify subgroups with distinct clinical outcomes and high risk of AML transformation of myelodysplastic syndrome. Blood 2009;114:1063–72. [PubMed: 19443663]

32. Leong HS, Kipling D. Text-based over-representation analysis of microarray gene lists with annotation bias. Nucleic Acids Res 2009;37: e79. [PubMed: 19429895]

33. Bagger FO, Sasivarevic D, Sohi SH, et al. BloodSpot: a database of gene expression profiles and transcriptional programs for healthy and malignant haematopoiesis. Nucleic Acids Res 2016;44:D917–24. [PubMed: 26507857]

34. Fisher R On the "probable error" of a coefficient of correlation deduced from a small sample. Metron 1921;1:32.

35. Wegner KW, Saleh D, Degterev A. Complex pathologic roles of RIPK1 and RIPK3: Moving beyond necroptosis. Trends Pharmacol Sci 2017;38:202–25. [PubMed: 28126382]

36. Tsoplou P, Kouraklis-Symeonidis A, Thanopoulou E, Zikos P, Orphanos V, Zoumbos NC. Apoptosis in patients with myelodysplastic syndromes: differential involvement of marrow cells in 'good' versus 'poor' prognosis patients and correlation with apoptosis-related genes. Leukemia 1999;13:1554–63. [PubMed: 10516757]

37. Lepelley P, Campergue L, Grardel N, Preudhomme C, Cosson A, FenauxP. Is apoptosis a massive process in myelodysplastic syndromes? Br J Haematol 1996;95:368–71. [PubMed: 8904894]

38. Hellstrom-Lindberg E, Kanter-Lewensohn L, Ost A. Morphological changes and apoptosis in bone marrow from patients with myelodysplastic syndromes treated with granulocyte-CSF and erythropoietin. Leuk Res 1997;21:415–25. [PubMed: 9225069]

39. Degterev A, Hitomi J, Germscheid M, et al. Identification of RIP1 kinase as a specific cellular target of necrostatins. Nat Chem Biol 2008;4:313–21. [PubMed: 18408713]

40. Mestrum SGC, de Wit NCJ, Drent RJM, Hopman AHN, Ramaekers FCS, Leers MPG. Proliferative activity is disturbed in myeloproliferative neoplasms (MPN), myelodysplastic syndrome (MDS), and MDS/MPN diseases: differences between MDS and MDS/MPN. Cytometry B Clin Cytom 2021;100:322–30. [PubMed: 32857909]

41. Shah S, Mudireddy M, Hanson CA, et al. Marked elevation of serum lactate dehydrogenase in primary myelofibrosis: clinical and prognostic correlates. Blood Cancer J 2017;7:657. [PubMed: 29249804]

42. Sallman DA, List A. The central role of inflammatory signaling in the pathogenesis of myelodysplastic syndromes. Blood 2019;133:1039–48. [PubMed: 30670444]

43. Bedoui S, Herold MJ, Strasser A. Emerging connectivity of programmed cell death pathways and its physiological implications. Nat Rev Mol Cell Biol 2020;21:678–95. [PubMed: 32873928]

44. Malireddi RKS, Gurung P, Mavuluri J, et al. TAK1 restricts spontaneous NLRP3 activation and cell death to control myeloid proliferation. J Exp Med 2018;215:1023–34. [PubMed: 29500178]

45. Lawlor KE, Khan N, Mildenhall A, et al. RIPK3 promotes cell death and NLRP3 inflammasome activation in the absence of MLKL. Nat Commun 2015;6:6282. [PubMed: 25693118]

46. Li H, Zhu H, Xu CJ, Yuan J. Cleavage of BID by caspase 8 mediates the mitochondrial damage in the Fas pathway of apoptosis. Cell 1998;94:491–501. [PubMed: 9727492]

47. Declercq W, Vanden Berghe T, Vandenabeele P. RIP kinases at the cross-roads of cell death and survival. Cell 2009;138:229–32. [PubMed: 19632174]

Author Manuscript

Author Manuscript

Author Manuscript

Author Manuscript

## HIGHLIGHTS

- Programmed necroptosis is increased in MDS as suggested by increased RIPK1 in erythroid precursors.

- Programmed necroptosis contributes to ineffective hematopoiesis in MDS.

- Inhibiting RIPK1 improves erythroid colony-forming ability of human MDS.
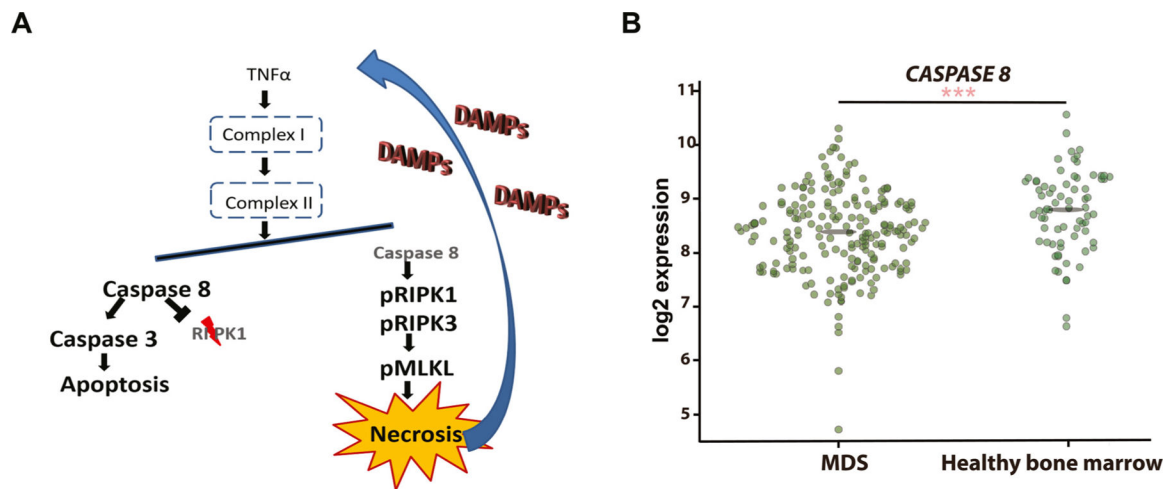
**Figure 1.**

*CASPASE-8* expression was lower in MDS as compared with healthy bone marrow in the MILE data set. **(A)** Activated caspase-8 cleaves and inactivates RIPK1 and RIPK3, thereby preventing necroptosis and triggering apoptosis. However, if caspase-8 enzymatic activity is inhibited (by cFLIP), RIPK1 and RIPK3 are stabilized and form the necroptosome, eventually resulting in necroptosis. **(B)** Gene expression among cell death pathways was analyzed using the publicly available microarray data GSE15061. *CASPASE-8* expression was significantly lower in the bone marrow of 164 patients with MDS versus that of 68 healthy controls ($p = 0.0000109$).
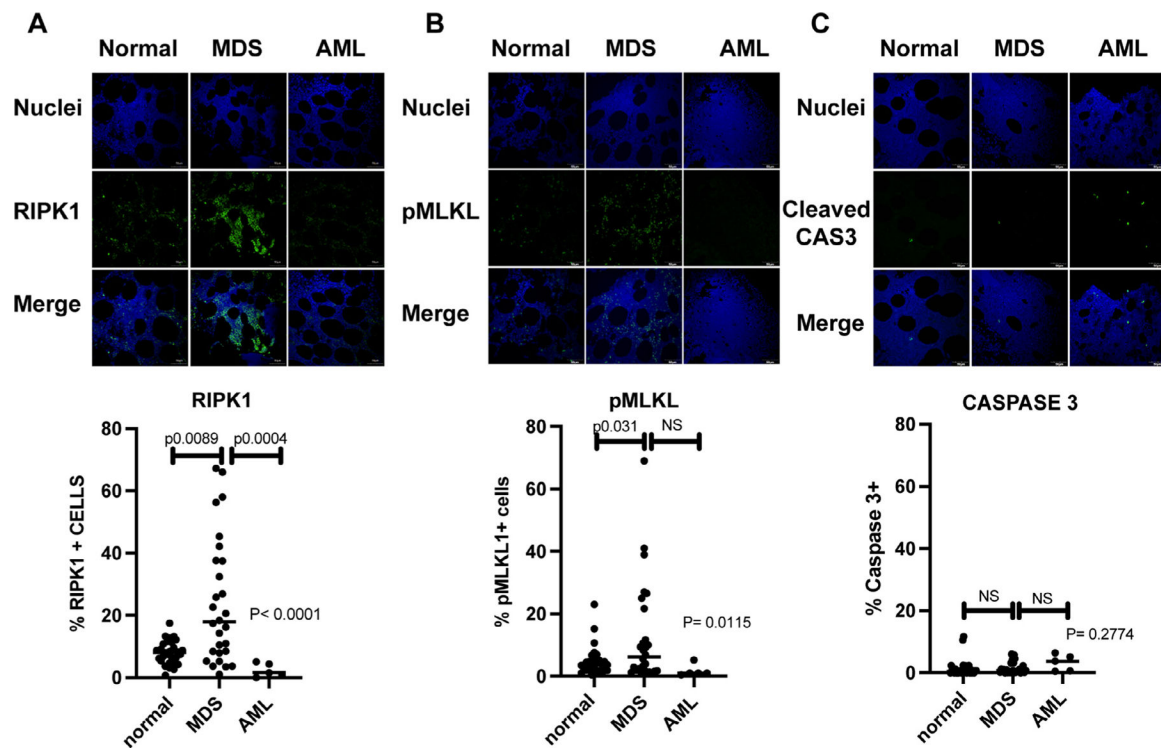
**Figure 2.**
Expression of RIPK1 and pMLKL, but not cleaved caspase-3, was increased in the bone
marrow of patients with MDS relative to control patients or patients with de novo AML. **(A)**
Confocal images of immunofluorescence (IF) staining for RIPK1 (*green*) and nuclei (*blue*)
of bone marrow (BM) core tissue sections obtained from either control patients or patients
with MDS or de novo AML. Bars = 50 $\mu$m. RIPK1$^+$ cells have been counted on scanned
images of whole slides from all control patients, MDS patients, and de novo AML patients.
There were significant differences in the percentages of RIPK1$^+$ cells between control
patients and MDS patients (p = 0.0089), and control patients and de nova AML patients (p
= 0.0004). **(B)** Confocal images of IF staining for pMLKL (*green*) and nuclei (*blue*) of BM
core tissue sections obtained from all patients. Bars = 50 $\mu$m. pMLKL$^+$ cells were counted
on scanned images of whole slides from all control, MDS and de novo AML patients. The
percentage of pMLKL$^+$ cells differed significantly between MDS and control patients (p =
0.031). **(C)** Confocal images of immunofluorescence staining for cleaved caspase-3 (*green*)
and nuclei (*blue*) of BM core tissue sections obtained from either control, MDS or de novo
AML patients. Bar = 50 $\mu$m. Cleaved caspase-3 expression did not differ among the three
groups. The lines indicate mean value and standard error (SE) of each group.
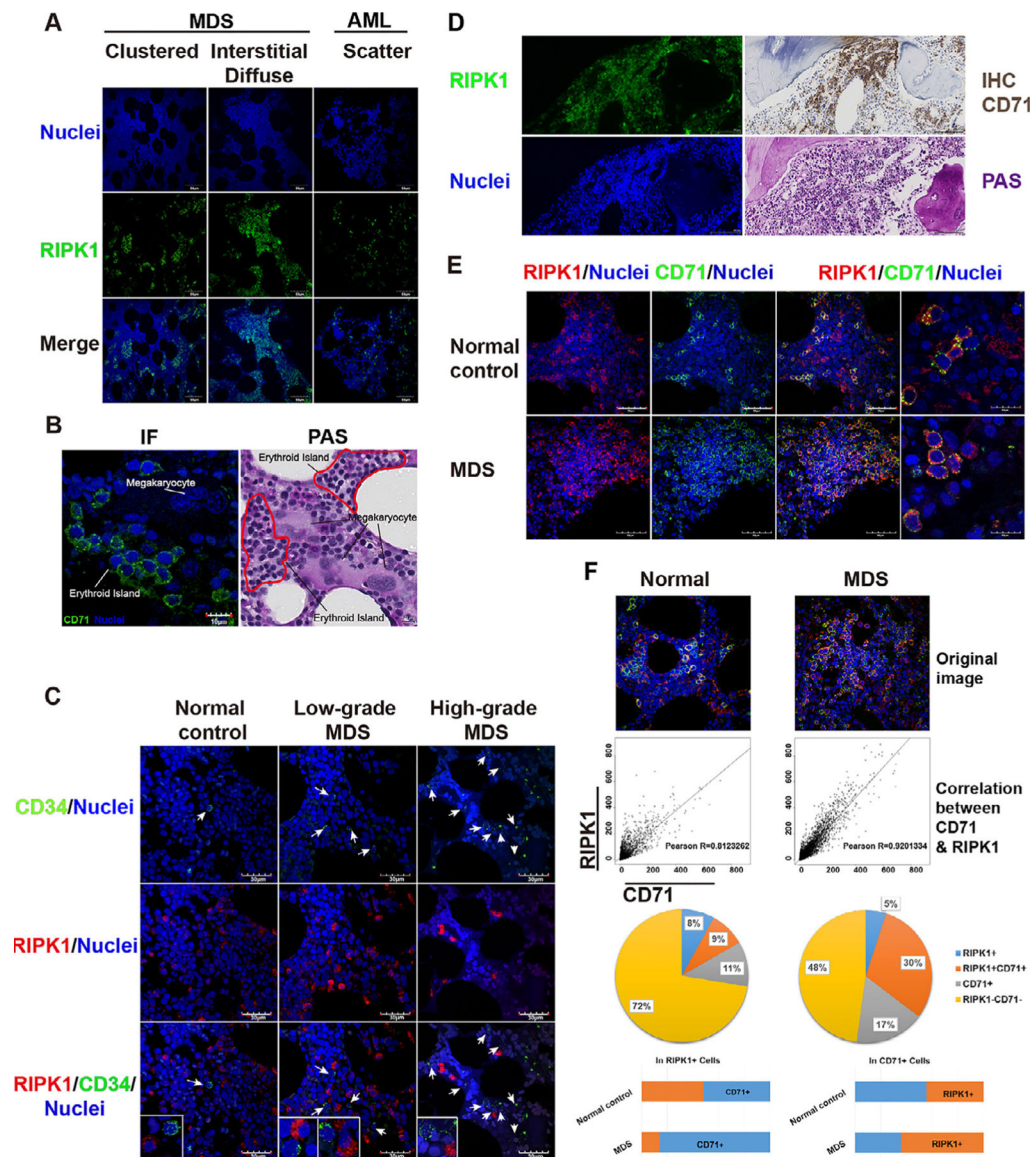
**Figure 3.**
RIPK1$^+$ cells were highly correlated with CD71$^+$ but not CD34$^+$ cells. **(A)** RIPK1$^+$ cells (*green*) were mononuclear cells arranged primarily in clusters in MDS but scattered in AML samples. Bars = 50 $\mu$m. **(B)** Confocal image of human bone marrow erythroid islands marked with immunofluorescence (IF) staining of CD71$^+$ cells (*green*). In periodic acid–Schiff (PAS)-stained slides, clusters of developing erythroid precursors, the erythroid islands, can be found in proximity to the marrow sinusoids. Bars = 10 $\mu$m. **(C)** Multiplex IF staining of normal, low-grade, and high-grade MDS BM core tissue sections with CD34 (*green*), RIPK1 (*red*), and 4′,6-diamidino-2-phenylindole (DAPI; nuclei, *blue*). In both control patient and MDS samples, RIPK1$^+$ cells did not exhibit CD34 staining. Bars = 30 $\mu$m. **(D)** Sequential sections representing the same level of tissue from an MDS BM sample. IF staining with RIPK1 (*green*) and DAPI (*blue*), immunohistochemical staining with CD71, and PAS. RIPK1 and CD71 signals were highly colocalized. Bars = 100 $\mu$m. **(E)** Multiple IF

staining of normal and MDS BM core tissue sections with CD71 (*green*), RIPK1 (*red*) and DAPI (nuclei, *blue*). In both control and MDS samples, RIPK1$^+$ cells were highly correlated with CD71$^+$ cells. Bars = 50 $\mu$m. (**F**) CellProfiler analysis of the multiplex IF images. Analysis of CD71 and RIPK1 staining in the control and MDS groups revealed a strongly positive correlation. Control: $R^2$ = 0.6599, Pearson's $R$ = 0.8123, $p < 0.0001$. MDS: $R^2$= 0.8366, Pearson's $R$ = 0.9201, $p < 0.0001$. To test the difference between the correlation in the control and MDS groups, we used the procedure developed by Fisher [34] ($p < 0.0001$), leading to the conclusions that the correlation of RIPK1 staining with CD71 staining in MDS is significantly higher than in the control group.
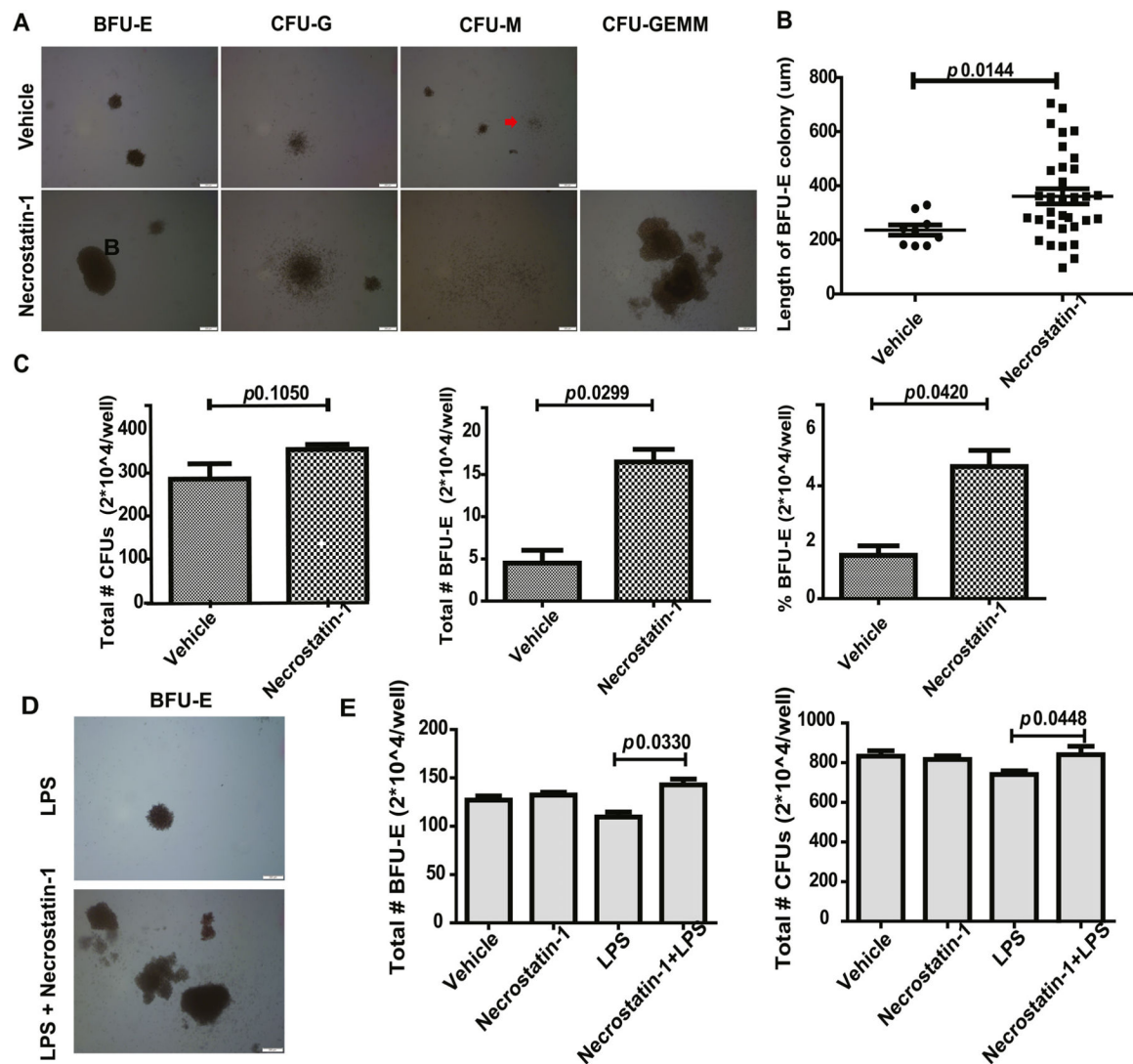
**Figure 4.**
MDS–MLD patient BM has increased size and number of burst-forming unit—erythroid (BFU-E) colonies in the presence of necrostatin-1. **(A)** MDS MDS-MLD patient bone marrow was cultured in methylcellulose in the presence of vehicle (DMSO, 1 $\mu$L/mL) or necrostatin-1 (25 $\mu$mol/L). Colonies were identified by morphology on day 12 and counted. Images are of BFU-E, CFU-G, CFU-M, and CFU-GEMM. Bar = 200 $\mu$m. **(B)** Quantitation of the length of BFU-E colonies with vehicle (dimethyl sulfoxide, 1 $\mu$L/mL) or necrostatin-1 (25 $\mu$mol/L). The length reported is the diameter of the colony measured at the longest dimension. **(C)** Total number of colonies (CFUs) and total number and percentage of BFU-E with vehicle (DMSO, 1 $\mu$L/mL) or necrostatin-1 (25 $\mu$mol/L). **(D)** Image of BFU-E colonies of normal apheresis monocytes treated for 5 hours with vehicle (DMSO 1 $\mu$l/mL), LPS (10 $\mu$g/mL), necrostatin-1 (25 $\mu$mol/L), and LPS (10 $\mu$g/mL) + necrostatin-1 (25 $\mu$mol/L) for 5 hours and grown in methylcellulose. Colonies were identified by morphology and counted on day 8. BFU-E colonies grown in methylcellulose with vehicle (DMSO, 1 $\mu$L/mL) or necrostatin-1 (25 $\mu$mol/L) in the presence of LPS (10 $\mu$g/mL) as described for normal human

apheresis. **(E)** Quantitation of the number of total BFU-E colonies and total CFU-E colonies of normal mononuclear apheresis cells treated with vehicle, LPS (10 $\mu$g/mL), and LPS (10 $\mu$g/mL) + necrostatin-1 (25 $\mu$mol/L) for 5 hours and grown in methylcellulose. Colonies were counted on day 8. $n$ = number of colonies counted.
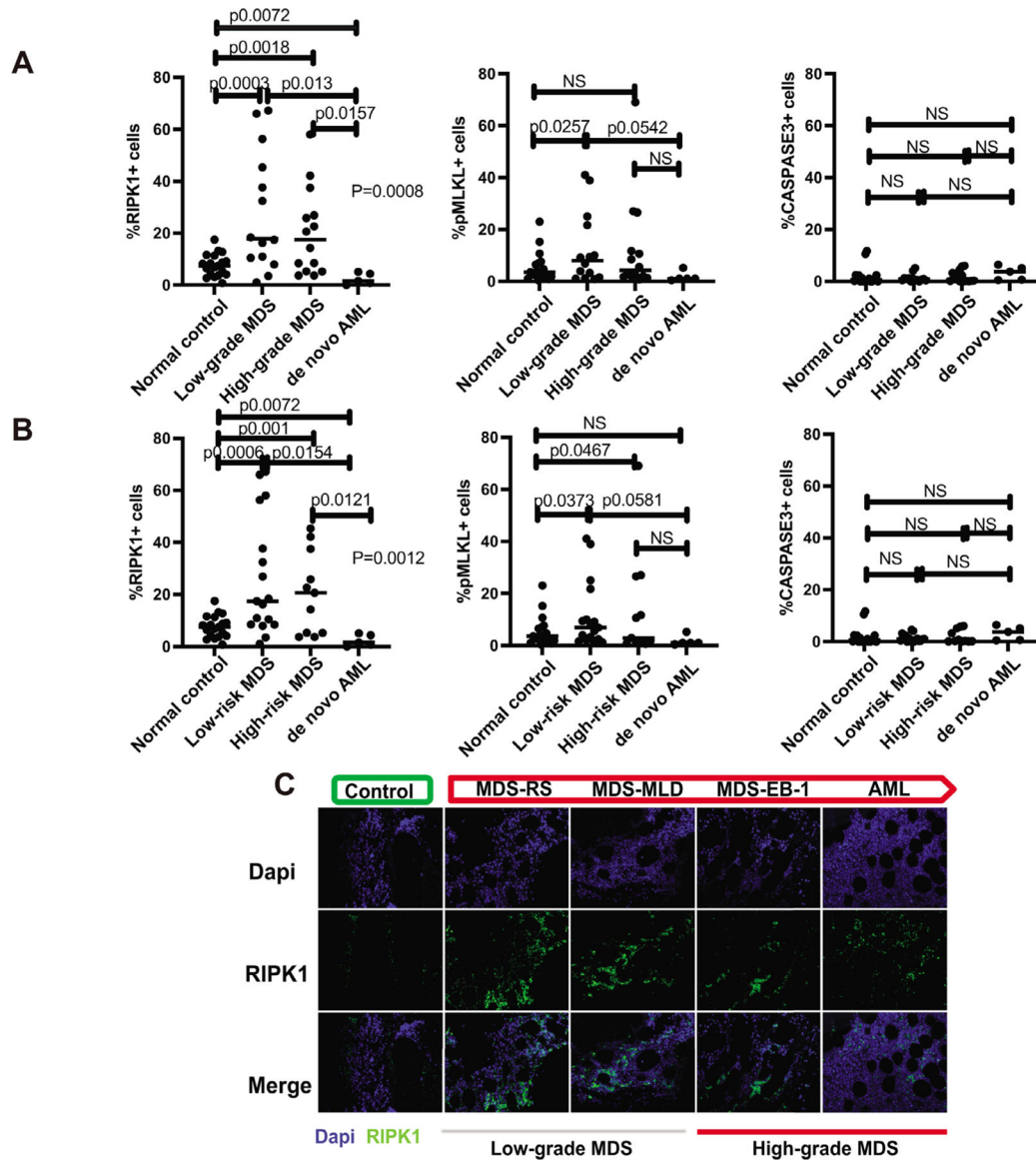
**Figure 5.**
RIPK1 expression is increased in cases with low-grade morphology and low IPSS-R scores. **(A)** The MDS group was divided into low-grade (BM blast <5%) and high-grade (BM blast 5% - <20%). The proportion of RIPK1+ cells differed significantly between control patients and patients with low-grade MDS ($p = 0.0003$). Likewise, RIPK1 staining was less common in patients with de novo AML than in patients with low-grade MDS ($p = 0.013$), patients with high-grade MDS ($p\ 0.0157$) or control patients ($p = 0.0072$). The proportion of pMLKL+ cells was significantly different between control patients and patients with low-grade MDS ($p = 0.0257$); pMLKL staining was less common in de novo AML than in low-grade MDS ($p = 0.0542$). There was no significant difference in pMLKL expression between control patients and patients with high-grade MDS. To evaluate apoptosis, we performed cleaved caspase-3 staining on the same samples. There was no difference in the proportion of caspase-3$^+$ cells among the control patients, and patients with low-grade MDS,

high-grade MDS or de novo AML. **(B)** The MDS group was divided into low-risk (IPSS-R score 4.5) and high-risk (IPSS-R score>4.5) subgroups. The proportion of RIPK1$^+$ cells differed significantly between control patients and patients with low-risk MDS ($p$ =0.0006), between control patients and patients with high-risk MDS ($p$ = 0.001), between patients with de novo AML and those with low-risk MDS ($p$ = 0.0154), between patients with de novo AML and high-risk MDS ($p$ = 0.0121), and between patients with de novo AML and control patients (p-0.0072). The proportion of pMLKL$^+$ cells in control patients was less than in low-risk MDS ($p$ =0.0373), and high-risk MDS ($p$ = 0.0467). There was no difference in the proportion of caspase-3$^+$ cells among the control, low-risk MDS, high-risk MDS and de novo AML groups. **(C)** Longitudinal data from a patient with MDS (MDS-MLD). RIPK1 is high in low-grade MDS and decreases on progression to high-grade MDS and AML.

## A  MDS vs. AML

| Symbol | Log2 Fold Change | p- value |
|---|---|---|
| FAS | 0.184036 | 6.33E-04 |
| FADD | 0.076191 | 1.25E-04 |
| TRADD | 0.088353 | 1.80E-09 |
| CFLAR (FLIP) | 0.100897 | 1.31E-07 |
| RIP1 | 0.037263 | 1.48E-03 |
| RIP3 | 0.082442 | 1.56E-05 |
| MLKL | 0.174587 | 7.78E-25 |
| BID | -0.04669 | 3.57E-05 |
| BAX | -0.10137 | 1.00E-07 |
| BAK1 | -0.19971 | 2.08E-22 |
| BAD | -0.14062 | 1.49E-13 |
| BCL2 | -0.4668 | 2.13E-27 |
| BCL2L2(BCL-W) | -0.13675 | 9.48E-21 |
| BCL2L11(Bim) | 0.174418 | 4.76E-12 |
| BCL2L1(BCL-XL) | 0.058884 | 3.29E-03 |
| MCL-1 | -0.28596 | 4.81E-11 |
| CYCS | -0.42083 | 3.27E-16 |
| CASPASE 8 | -0.20869 | 1.74E-07 |
| CASPASE 9 | -0.0927 | 5.88E-14 |
| CASPASE 10 | 0.212051 | 2.55E-18 |
| CASPASE 3 | 0.06691 | 3.73E-06 |
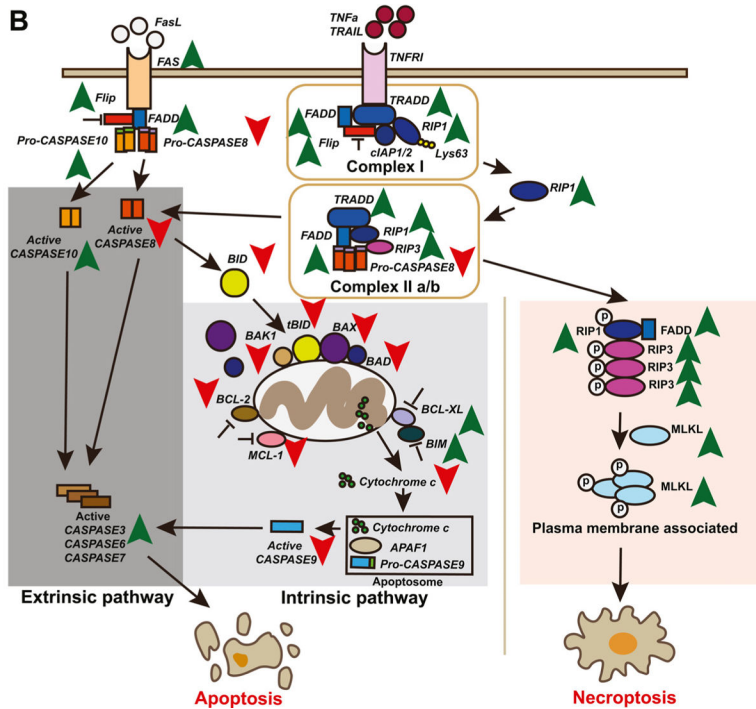


**Figure 6.**
The necroptosis pathway is activated in MDS: Reanalysis of the microarray gene expression data of the MILE data set (GSE15061). **(A)** Gene expression changes among the apoptosis and necroptosis pathways significantly differed between MDS and AML. The data are represented as $\log_2$-fold change. **(B)** Pictorial representation of (A). Analysis of the GSE15601 microarray data comparing 164 patients with MDS with 202 patients with AML. The necroptosis pathway was activated, and the intrinsic pathway was suppressed.

**Table 1**

Comparison of clinical data between normal controls, MDS and de novo AML patient cohorts.

| Variables | De novo AML (N=5) | MDS (N=28) | Normal controls (N=29) | P-value |
|---|---|---|---|---|
| Gender | | | | |
| female | 80% (4) | 39% (11) | 39% (12) | 0.5 |
| male | 20% (1) | 61% (17) | 61% (17) | |
| Age (years) | 60.48 ± 16.81 | 68.16 ± 9.56 | 52.72 ± 15.74 | 0.0003 |
| ANC ($10^3$/ul) | 0.812 ± 1.114 | 1.654 ± 2.101 | 4.303 ± 3.822 | 0.0026 |
| PLT ($10^3$/ul) | 104.4 ± 90.6 | 117.6 ± 84.17 | 196.5 ± 105.1 | 0.0063 |
| HB (g/dl) | 11.22 ± 2.86 | 9.11 ± 2.47 | 11.80 ± 2.154 | 0.0003 |
| Blasts (%) | 69.40 ± 22.87 | 4.74 ± 4.24 | 1.54 ± 1.52 | <0.0001 |
| Cytogenetics | | | | |
| Very good | 0 | 2 | 0 | – |
| Good | 4 | 13 | 29 | – |
| Intermediate | 0 | 8 | 0 | – |
| Poor | 0 | 4 | 0 | – |
| Very poor | 1 | 1 | 0 | – |
| IPSS-R score | | | | |
| Very low | – | 2 | – | – |
| Low | – | 7 | – | – |
| Intermediate | – | 8 | – | – |
| High | – | 7 | – | – |
| Very high | – | 4 | – | – |

x ± s represents X ± 1SD. N is the number of non-missing variables. Numbers after proportions are frequencies.

Pearson test used for gender; Kruskal-Wallis test used for age, ANC, PLT, HB, Blasts.